JOURNAL OF SPACECRAFT AND ROCKETS
Vol. 31, No. 6, November–December 1994

Safety Index Approach to Predicting the Storage Life of Rocket Motors

I. Janajreh,* R. A. Heller,† and S. Thangjitham‡
Virginia Polytechnic Institute and State University, Blacksburg, Virginia 24061-0219

The first-order second-moment reliability method is used to predict the service life of rocket motors subjected to environmental temperature variations. All mechanical and thermal variables have statistical variations and correlation between variables, specifically between strength and modulus, as well as various distribution functions such as normal, lognormal, and Weibull.

Nomenclature

A_d, A_y	= temperature amplitudes, daily and yearly
A_E, B_E, β_E	= parameters for viscoelastic modulus, aging factor
A_R, B_R, β_R	= parameters for strength, aging factor
a_t	= viscoelastic shift function
B, C	= damage parameters
Br, Kr	= Kelvin functions
$[C]$	= covariance matrix
C_j^1, C_j^2	= Constants for temperature frequency response function
D	= damage factor
E_i, E_∞	= moduli for Maxwell elements, rest modulus, psi
E_j	= modulus of the jth layer, psi
$E(T, \omega), E'(T, \omega)E''(T, \omega)$	= moduli: complex, storage, and loss
$F_x(.)$	= probability function of variable x
$f_x(.)$	= density function of variable x
G	= performance function
j	= index for jth layer
k_j	= thermal diffusivity of the jth layer
$L(t)$	= reliability to time t
P_{fk}	= probability of failure at the kth day
$P_f(t)$	= progressive probability of failure to time t
R	= mean strength
R_0, n	= mean strength parameters
r, r_j	= radial coordinate, outer radius of the jth layer
$S_r(r, \omega), S_\theta(r, \omega)$	= stress frequency response functions, radial and tangential, psi/F°
$S_\theta(r, t)$	= tangential stress, psi
T, T_f, T_m	= temperature, stress-free temperature, and mean temperature
$\bar{T}_j$	= temperature frequency response function of the jth layer
t	= time
$\{x\}$	= vector of random variables
x_i^*	= value of the random variable x_i at the failure point
x_0, x_c, m	= parameters for Weibull distribution function
$\{y\}$	= vector of uncorrelated normal random variables
$\hat{\alpha}_i$	= direction cosine for the random variable x_i
α_j	= coefficient of thermal expansion for the jth layer
$\bar{\alpha}_j$	= thermal diffusivity for the jth layer
β, β_k	= safety index and safety index at the kth day
$\Gamma(.)$	= gamma function
Δt	= time step, 24 h
η_R, η_E	= aging factors, strength and modulus
θ	= tangential coordinate
$\lambda_x, \zeta_x, \hat{x}$	= parameters for lognormal distribution function
λ_1, λ_2	= eigenvalues
μ_{xi}, σ_{xi}	= mean and standard deviation for x_i
ν_j	= Poisson's ratio for the jth layer
ρ	= correlation coefficient
τ_i	= relaxation time, hrs
$\Phi(.)$	= normal probability function
$[\Phi], [\Phi]^T$	= modal matrix and modal matrix transpose
ϕ_d, ϕ_y	= phase angles, daily and yearly
ϕ_1, ϕ_2	= components of an eigenvector
$\phi(.)$	= normal density function
$\omega, \omega_d, \omega_y$	= frequency, daily frequency, and yearly frequency

Received Nov. 13, 1991; revision received June 30, 1992; accepted for publication July 10, 1992.

*Research Assistant, Department of Engineering Science and Mechanics.
†Professor, Department of Engineering Science and Mechanics. Associate Fellow AIAA.
‡Associate Professor, Department of Engineering Science and Mechanics.

Introduction

STORAGE life of rocket motors has been discussed in several papers, using various reliability techniques. In this paper, the first-order second-moment (FOSM) reliability method is used to predict the service life of rocket motors. This technique allows different probability distributions for each variable and allows for dependence between variables in terms of correlation.

FOSM requires the availability of the first two moments, mean and variance, of a variable from which a safety index is calculated. Using a series of transformations, variables are normalized and decoupled, and probabilities of failure are determined as functions of service loads based on tangential and radial thermal stresses.

Motors are considered to be long hollow elastic cylindrical shells, surrounded by a layer of insulation and filled with a viscoelastic propellant whose strength is degraded by cumulative damage and aging. Temperature is symmetric with respect to the axis of the motor, and the outside surface temperature is the same as air temperature.

Before the induced thermal stresses are calculated at a certain point in the motor, the temperature at that point must be known.

Hence the first task is to determine the temperature at the instant at which the stresses are desired, and the second one is to compute the stresses themselves.

In previous studies,[1-5] a recorded time series of actual hourly temperatures has been used as an input. Such a detailed series has been found to be unnecessarily costly in terms of computer time. In the present analysis only seasonal and diurnal temperature variations are considered without significant loss of accuracy and considerable savings in computational costs.

Thermal Stress Analysis

Though the thermal stress analysis of a layered cylinder has been presented in many papers,[1-5] it is repeated here in a shortened form for the sake of completeness.

Assuming an axisymmetric temperature distribution around the cylinder, the heat conduction equation in cylindrical coordinates is used for each layer (see Fig. 1):

$$\frac{\partial^2 T_j}{\partial^2 r} + \frac{1}{r}\frac{\partial T_j}{\partial r} = \frac{1}{\bar{\alpha}_j}\frac{\partial T_j}{\partial t} \tag{1}$$

The temperature of the jth layer, $T_j(r, t)$, is a function of both radial coordinate r and time t. Using the frequency response function approach, the temperature can be written as

$$T_j(r, t) = \bar{T}_j(r, \omega)e^{i\omega t} \tag{2}$$

Substituting Eq. (2) into Eq. (1) the solution of Eq. (1) becomes

$$\bar{T}_j(r, \omega) = C_j^1 Br(x_j) + C_j^2 Kr(x_j) \tag{3}$$

where $x_j = \sqrt{\omega/\bar{\alpha}_j r_j}$, and C_j^1 and C_j^2 are coefficients to be determined from the following boundary conditions:

1) The temperature at the center is finite.
2) The temperatures are the same on both sides of an interface.
3) The heat flux across an interface is continuous.
4) The temperature on the surface of the fifth layer varies sinusoidally with a unit amplitude and a frequency ω. Although temperature is evaluated in all five layers, stresses are of interest only in layers 2 and 3.

The frequency response function of the temperature is used to evaluate the frequency response functions for the stress components $S_r(r, \omega)$ and $S_\theta(r, \omega)$ for the following boundary conditions: continuity of radial displacements and radial stresses on interfaces and zero radial stresses on the bore and the external surface of layer 3.

Because storage life is limited by the deterioration of the propellant rather than the case, only stresses in the second layer (propellant) are evaluated. These are given as

$$S_r(r, \omega) = \frac{r_2^2}{r_2^2 - r_1^2}\left(1 - \frac{r_1^2}{r^2}\right)E_2\frac{q_1}{q_2} + \frac{\alpha_2 E_2}{(1-\nu_2)(r_2^2 - r_1^2)}\left(1 - \frac{r_1^2}{r^2}\right)\int_{r_1}^{r_2}\bar{T}_2(r, \omega)r\,\mathrm{d}r - \frac{\alpha_2 E_2}{(1-\nu_2)r^2}\int_{r_1}^{r}\bar{T}_2(r, \omega)r\,\mathrm{d}r \tag{4}$$

$$S_\theta(r, \omega) = -\frac{r_2^2}{r_2^2 - r_1^2}\left(1 + \frac{r_1^2}{r^2}\right)E_2\frac{q_1}{q_2} + \frac{\alpha_2 E_2}{(1-\nu_2)(r_2^2 - r_1^2)}\left(1 + \frac{r_1^2}{r^2}\right)\int_{r_1}^{r_2}\bar{T}_2(r, \omega)r\,\mathrm{d}r + \frac{\alpha_2 E_2}{(1-\nu_2)r^2}\int_{r_1}^{r}\bar{T}_2(r, \omega)r\,\mathrm{d}r - \frac{\alpha_2 E_2 \bar{T}_2(r, \omega)}{1-\nu_2} \tag{5}$$

where

$$q_1 = 2\alpha_2(1+\nu_2)\int_{r_1}^{r_2}\bar{T}_2(r, \omega)r\,\mathrm{d}r - \alpha_3(1+\nu_3)\left(r_2^2 - r_1^2\right)\bar{T}_2(r_2, \omega)$$

$$q_2 = (1+\nu_2)(1-2\nu_2)r_2^2 + (E_2/E_3)(1-\nu_3^2)r_2\left(r_2^2 - r_1^2\right)/(r_3 - r_2)$$

The stress frequency response functions, Eqs. (4) and (5), are complex quantities. Their magnitudes are obtained as

$$|S(r, \omega)| = \left[S^2(r, \omega)_{\mathrm{RE}} + S^2(r, \omega)_{\mathrm{IM}}\right]^{1/2}$$

They are the response to a sinusoidal temperature input of unit amplitude and frequency ω. A temperature input consists of several constant and sinusoidal components:

$$T = T_f - [T_m + A_y\sin(\omega_y t + \phi_y) + A_d\sin(\omega_d t + \phi_d)] \tag{6}$$

Calculations indicate that the tangential stress at the bore is significantly greater than the radial stress at the bond line. Therefore only the time-dependent tangential stress will be considered. This can be written as

$$S_\theta(r, t) = T_f S_\theta(r, 0) - T_m S_\theta(r, 0) - A_d\sin(\omega_d t + \phi_d)S_\theta(r, \omega_d) - A_y\sin(\omega_y t + \phi_y)S_\theta(r, \omega_y) \tag{7}$$

Viscoelastic Properties of the Propellant

Both modulus and strength of the material are time- and temperature-dependent properties.

Since in storage thermal loads are essentially cyclic in nature, it is expedient to convert the time-dependent relaxation modulus into the frequency-dependent complex modulus representation. This is accomplished by performing sine and cosine Fourier transformations that yield a real and an imaginary term

$$E'(T, \omega)_{\mathrm{RE}} = E_\infty + \sum_{i=1}^{8}\frac{E_i\omega^2 a_t^2\tau_i^2}{1 + \omega^2\tau_i^2 a_t^2} \tag{8}$$

and

$$E''(T, \omega)_{\mathrm{IM}} = 2\pi\sum_{i=1}^{8}\frac{E_i\omega a_t\tau_i}{1 + \omega^2\tau_i^2 a_t^2} \tag{9}$$

Hence

$$E(T, \omega) = E'(T, \omega) + iE''(T, \omega)$$

and for the seasonal and diurnal frequencies the imaginary part can be neglected.[2]

In Eqs. (8) and (9), E_i and τ_i are moduli and relaxation times for parallel Maxwel elements,[3] and a_t for the material under investigation can be written as[4]

$$\log a_t = 1.42\left[-\frac{8.86(T + 34.0)}{181.9 + (T + 34.0)} + 3.32\right] \tag{10}$$

with T in degrees Fahrenheit. Substituting Eq. (10) into Eq. (8), one can compute the daily modulus as a function of temperature.

The mean strength $R(T, t)$ (psi) of a viscoelastic material is given in Ref. 5 as

$$R(T, t) = R_0\left(\frac{t}{4a_t}\right)^{-n}$$

For the propellant under consideration, $n = 0.0857$ and $R_0 = 139$ when t is measured in minutes, and $R_0 = 98$ when t is in hours. Experiments conducted by the U.S. Army Missile Command[6] indicate that the bond line strength for room temperature and above is approximately twice as high as the tensile strength of the propellant. Only at low temperatures is the bond line weaker than the propellant. At 0°F their ratio is 0.8.

Cumulative Damage and Aging

The linear cumulative damage rule proposed by Ref. 8 states that damage produced in time spent at a particular stress level S_i is inversely proportional to the time t_{fi} required to produce failure in the material at that stress level:

$$d_i = 1/t_{fi}$$

The total damage produced by N stress levels is

$$D = \sum_{i=1}^{N} t_i/t_{f_i} \tag{11}$$

where t_i is the duration for each stress level. A relationship between constant stress and reduced time to failure is given as

$$t_{fi}/a_t = C S_i^{-B}$$

where C and B are material parameters ($C = 1.6 \times 10^{16}$ and $B = 8.76$ are being used here). The cumulative damage D becomes

$$D = \frac{1}{C}\sum_{i=1}^{n} \frac{S_i^B t_i}{a_t} \tag{12}$$

Therefore, the degraded mean strength can be written as

$$R'(T, t) = R(T, t)(1 - D)$$

Aging is defined as the change in physical and thermal parameters in an unloaded condition. It is accelerated in warm climates and during summer periods. It has been shown that the ratio $\eta(T, t)$ of the current value of a property to its initial value is proportional to the logarithm of time.[8,9]

In the case of strength

$$\eta_R(T, t) = \frac{R(T, t)}{R(T, 0)} = 1 - \beta_R(T)\log t \tag{13}$$

where the coefficient $\beta_R(T)$ is an exponentially decreasing function of absolute temperature T. Hence,

$$\beta_R(T) = A_R e^{-B_R/T} \tag{14}$$

$$R(T, t) = \eta_R R_0 \left(\frac{t}{a_t}\right)^{-m} \tag{15}$$

Here $A_R = 1.15 \times 10^{10}$ and $B_R = 1.53 \times 10^4$ with t in days and T in degrees Rankin.

In the case of the modulus E_2, the coefficients of Eqs. (14) and (15) are replaced by $A_E = 4.1 \times 10^5$ and $B_E = 8.75 \times 10^3$.

Variable temperature aging will be calculated based on the concept of reduced time.[8,9] If the propellant is aged at temperature T_1 for the period of t_1 days, the aging factor becomes equal to

$$\eta_1 = 1 - \beta_1 \log t_1 \tag{16}$$

where $\beta_1 = Ae^{-B/T_1}$. The same aging factor may be obtained at a different temperature T_2 in time t_1', called equivalent time. Hence the equivalent time during which the same aging parameter is reached at T_2 becomes equal to

$$t_1' = t_1^{\beta_1/\beta_2} \tag{17}$$

If aging is now continued at T_2 for an additional time Δt, the total aging time t_2 will be the sum

$$t_2 = t_1' + \Delta t \tag{18}$$

The process is then repeated for other temperatures.

Because the aging at practical service temperatures is relatively slow, it has been found that diurnal temperature variations have an insignificant effect on aging factors. As a consequence, only seasonal thermal changes have been included in aging calculations. Aging factors are evaluated for the average daily temperature.

First-Order Second-Moment Reliability Analysis

Failure of the motor takes place when the thermal stress exceeds the strength degraded by aging and cumulative damage. A performance function G is defined as

$$G = R - S_\theta \tag{19}$$

When $G \leq 0$, failure takes place. The probability of failure P_f is then given as

$$P_f = P[G \leq 0] \tag{20}$$

In general, the performance function is given in terms of several variables $\{x\}$,[10]

$$G = G(x_1, x_2, \ldots, x_i) \leq 0 \tag{21}$$

where x_i are uncorrelated reduced variates

$$x_i = \frac{x_i^* - \mu_{x_i}}{\sigma_{x_i}} \tag{22}$$

The safety index β is defined as the minimum length vector from the origin of the coordinate system of x_i to the performance function G:

$$|\beta| = \sqrt{x_1^2 + x_2^2 + \cdots + x_i^2} \tag{23}$$

The corresponding point x_i^* on G is called the design point. The direction cosines of β and $\hat{\alpha}_i$ are calculated from the partial derivatives of G:

$$\hat{\alpha}_i = \frac{\partial G}{\partial x_i^*}\sigma_{x_i} \Bigg/ \sqrt{\sum_{i=1}^{n}\left(\frac{\partial G}{\partial x_i}\sigma_{x_i}\right)^2} \tag{24}$$

A design value of the variables x_i^* is then obtained as

$$x_i^* = \mu_{x_i} - \hat{\alpha}_i \sigma_{x_i} \beta \tag{25}$$

These variables are substituted into the performance function, Eq. (19), and the equation is solved for β.

The process is iterative, in that the new values of x_i^* from Eq. (25) are used in evaluating an improved set of $\hat{\alpha}_i$ and subsequently a new value of β. In the absence of probability distributions for the variables, only the safety index β may be calculated.

Uncorrelated Normally Distributed Variables

When all variables are normally distributed, the safety index β will also be normal and the daily probability of failure may be obtained from the normal integral for the k^{th} day:

$$P_{fk} = \phi(-\beta_k) \tag{26}$$

Correlated Normally Distributed Variables

It has been observed that the strength and the modulus of solid propellant are correlated variables. Such interdependence is characterized by the correlation coefficient ρ

$$-1 < \rho < 1$$

The procedure in such circumstances requires a transformation to uncorrelated variables.[10]

In vector form the means and standard deviations become

$$\mu_x = \begin{pmatrix} \mu_{x_1} \\ \mu_{x_2} \end{pmatrix}, \qquad \sigma_x = \begin{pmatrix} \sigma_{x_1} \\ \sigma_{x_2} \end{pmatrix}$$

and the covariance matrix $[C]$ is

$$[C] = \begin{bmatrix} \sigma_{x_1}^2 & \rho\sigma_{x_1}\sigma_{x_2} \\ \rho\sigma_{x_1}\sigma_{x_2} & \sigma_{x_2}^2 \end{bmatrix} = \begin{bmatrix} \sigma_{x_1}^2 & C_{12} \\ C_{12} & \sigma_{x_2}^2 \end{bmatrix}$$

The two eigenvalues λ_1 and λ_2 and eigenvectors are determined next by solving the matrix equation

$$\begin{vmatrix} (\sigma_{x_1}^2 - \lambda) & C_{12} \\ C_{12} & (\sigma_{x_2}^2 - \lambda) \end{vmatrix} = 0$$

The eigenvectors are found from

$$\begin{bmatrix} (\sigma_{x_1}^2 - \lambda) & C_{12} \\ C_{12} & (\sigma_{x_2}^2 - \lambda) \end{bmatrix} \begin{pmatrix} \phi_1 \\ \phi_2 \end{pmatrix} = 0$$

From these a modal matrix $[\Phi]$ and its transpose $[\Phi]^T$ are obtained.

The means of the uncorrelated normal variables $\{y\}$ are calculated as

$$\bar{\mu}_y = \begin{pmatrix} \mu_{y_1} \\ \mu_{y_2} \end{pmatrix} = [\Phi]^T \begin{pmatrix} \mu_{x_1} \\ \mu_{x_2} \end{pmatrix}$$

and the standard deviations of these uncorrelated normal variables are

$$\sigma_y = \begin{pmatrix} \sigma_{y_1} \\ \sigma_{y_2} \end{pmatrix} = \begin{pmatrix} \sqrt{\lambda_1} \\ \sqrt{\lambda_2} \end{pmatrix}$$

For the calculation of the reliability index β, the technique described earlier can be used with some modifications. First the variables $\{x^*\}$ are transformed to uncorrelated variables

$$\{y\} = [\Phi]^T \{x^*\}$$

The derivatives of the performance function in terms of the uncorrelated variables are obtained as

$$\frac{\partial G}{\partial y} = [\Phi]^T \left\{ \frac{\partial G}{\partial x} \right\}$$

Next, the direction cosines $\{\hat{\alpha}\}$ are found

$$\{\hat{\alpha}\} = \left\{ \sigma_y \frac{\partial G}{\partial y} \bigg/ \sqrt{\sum_{i=1}^{n} \left(\sigma_{y_i} \frac{\partial G}{\partial y_i} \right)^2} \right\}$$

New values of $\{y\}$ are calculated:

$$y_i = \mu_{y_i} + \hat{\alpha}_i \beta \sigma_{y_i}$$

The original variables are obtained by the transformation

$$\{x^*\} = [\Phi]\{y\}$$

These are substituted into the performance function

$$G(x_1^*, x_2^*, \ldots, x_i^*) = 0$$

which is then solved for β. The process is repeated until convergence occurs.

Nonnormal Variables

When variables are not normally distributed, transformations to equivalent normal distributions are performed first. If the density function and probability distribution are $f_x(x^*)$ and $F_X(x^*)$, respectively, whereas the corresponding normal density and distribution at the design point are $\phi(x_i^*)$ and $\Phi(x_i^*)$, for equivalence

$$f_x(x^*) = \phi(x^*)$$

$$F_X(x^*) = \Phi(x^*)$$

The equivalent normal standard deviation is obtained from the relation

$$\sigma_x^N = \phi\left[\Phi^{-1}(F_X^*)\right] / f_x(x^*)$$

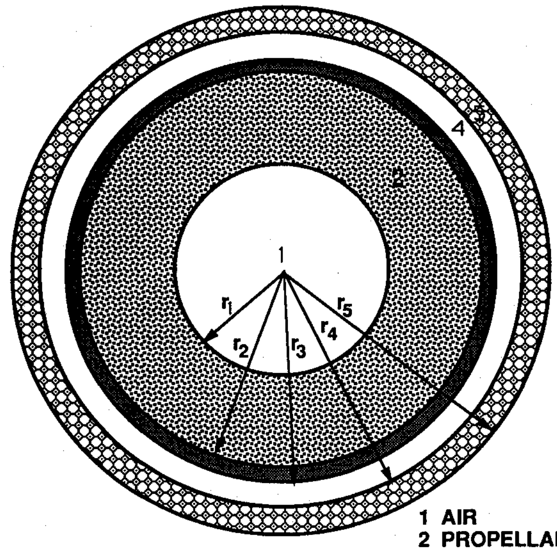

Fig. 1 Configuration of the solid propellant rocket motor.

and the normal mean from

$$\mu_x^N = X^* - \sigma_x^N \Phi^{-1}[F_X(x^*)]$$

These values are then used to replace the standard deviation and the mean in Eqs. (24) and (25). Then the probability of failure is calculated from Eq. (26).

Progressive Probability of Failure

The probabilities of failure calculated in the previous section lead to the concept of failure rate or hazard rate,[11] $h(t)$, which is the probability that a motor that survived to time t will fail during the next time unit. It is based on the application of a single stress and is defined as the ratio

$$h(t) = \frac{P_f(t)}{L(t)}$$

When a sequence of stresses is applied to the motor, its reliability $L(t)$ is calculated as

$$L(t) = \exp\left[-\int_0^t h(t)\,\mathrm{d}t \right]$$

In summation form

$$L(t_n) = \exp\left[-\sum_{j=1}^{n} \frac{P_f(t_j)}{L(t_{j-1})} \right] \tag{27}$$

with $L(0) = 1.0$

The progressive probability of failure is

$$P_f(t_j) = 1 - L(t_j) \tag{28}$$

Numerical Example

Evaluation of Stress and Strength

The motor configuration shown in Fig. 1 with geometric, thermal, and mechanical parameters presented in Table 1 has been analyzed. Coefficients of variation are given in the same table.

Three different locations are considered. Point Barrow, AK, represents a cold site; Yuma, AZ, represents a warm site; and Nashville, TN, represents a moderate site.

First, the frequency response function for temperature at the bore is evaluated for seasonal and diurnal frequencies, Eq. (3). Then the tangential bore stress is calculated based on Eqs. (5) and (7). Results are plotted in Fig. 2 for the three locations.

Table 1 Geometric, thermal, and mechanical parameters

Material	Air (core)	Propellant	δ	Case	δ	Air (gap)	Insulation
r, in.	1.875	4.302	—	4.400	—	5.400	6.400
Conductivity K, Btu/h ft °F	0.0145	0.7641	—	14.600	—	0.0145	0.0160
Diffusivity $\bar{\alpha}$, in.^{2}/h	109.872	4.378	—	48.960	—	109.872	1.235
Elastic modulus E and E_∞, psi	—	281.84	0.10	30.0×10^6	0.05	—	—
Poisson's ratio ν	—	0.492	0.0	0.253	0.05	—	—
Coefficient of thermal expansion α, in./in. °F	—	5.7×10^{-5}	0.05	6.5×10^{-6}	0.05	—	—
Strength	—	Eq. (13)	0.10	—	—	—	—
Stress-free temperature T_f, °F	—	165	—	—	—	—	—

Characteristics	Point Barrow, AK	δ	Nashville, TN	δ	Yuma, AZ	δ
Mean temperature T_m, °F	9.356	—	58.536	—	73.49	—
Daily amplitude A_d, °F	1.602	0.10	7.495	0.10	11.530	0.10
Yearly amplitude A_y, °F	30.690	0.10	20.678	0.10	19.224	0.10
ω_d	$2\pi/24$	—	$2\pi/24$	—	$2\pi/24$	—
ω_y	$2\pi/8760$	—	$2\pi/8760$	—	$2\pi/8760$	—
Daily phase ϕ_d	$15\omega_d$	—	$16\omega_d$	—	$16\omega_d$	—
Yearly phase ϕ_y	$5088\omega_y$	—	$4871\omega_y$	—	$4920\omega_y$	—

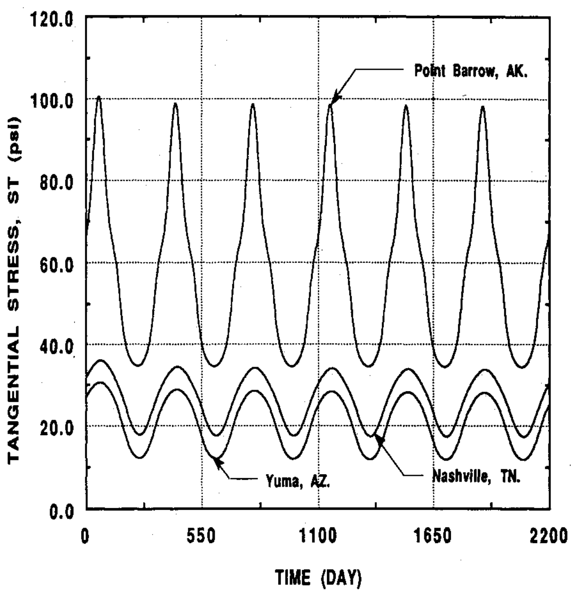

Fig. 2 Tangential stress ST at the bore due to cyclic temperature with time at different locations.

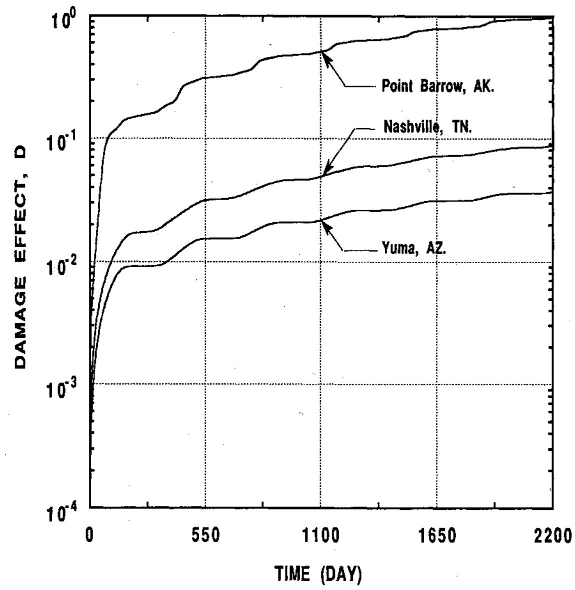

Fig. 3 Damage effect D on the strenth of the core at different locations.

The strength of the propellant is subject to cumulative damage as well as to chemical aging. Aging also affects the viscoelastic modulus. Cumulative damage is governed by Eqs. (11) and (12), whereas the aging parameters are calculated from Eqs. (13–18) along with the temperature history of Eq. (6).

Cumulative damage is presented in Fig. 3. The damage at Point Barrow becomes 1 after 2200 days, which corresponds to 0 strength, and further calculations are terminated. Aging factors are plotted in Fig. 4 for both strength and modulus. It is seen that the modulus and consequently the stresses are affected more by this phenomenon than is the strength of the material. Both indicate accelerated deterioration during the hot summer months. This explains why there is no aging effect on the strength at Point Barrow.

The seasonal variations of the modulus, including aging, are depicted in Fig. 5. The change in the slope is due to high variation of the modulus at low temperature levels. The plot presented in Fig. 2 indicates the seasonal changes in thermal stresses. The gradual deterioration of the core strength is seen in Fig. 6. The strength at Point Barrow becomes 0 after 2200 days, the same period in which the damage effect is 1.

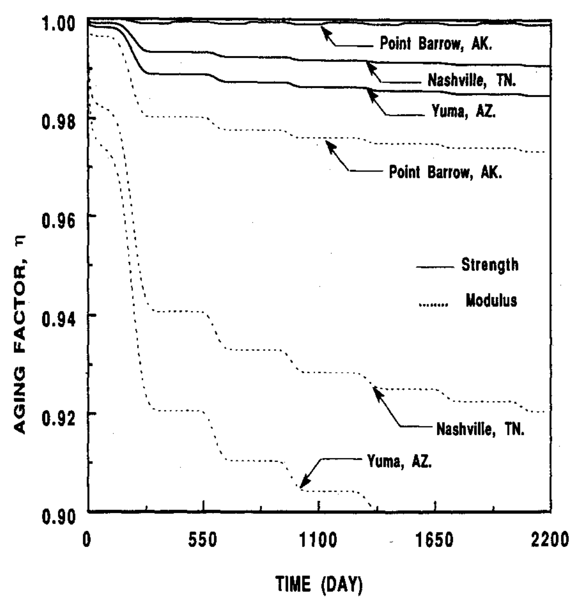

Fig. 4 Aging factor η with time at different locations.

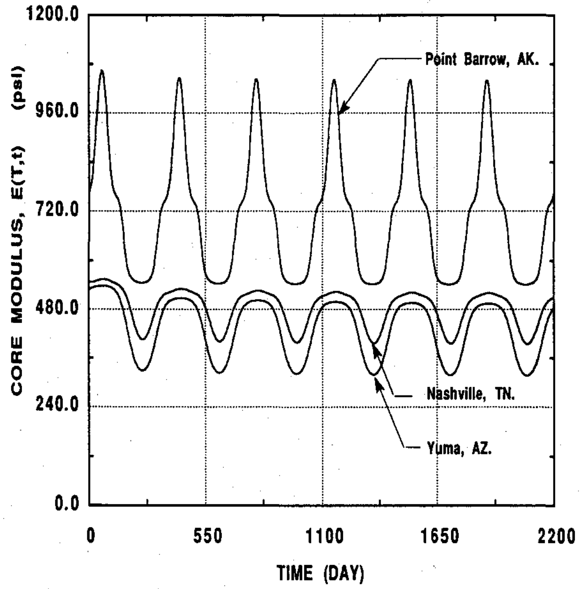

Fig. 5 Core modulus $E(T,t)$ with time at different locations (aging effects are included).

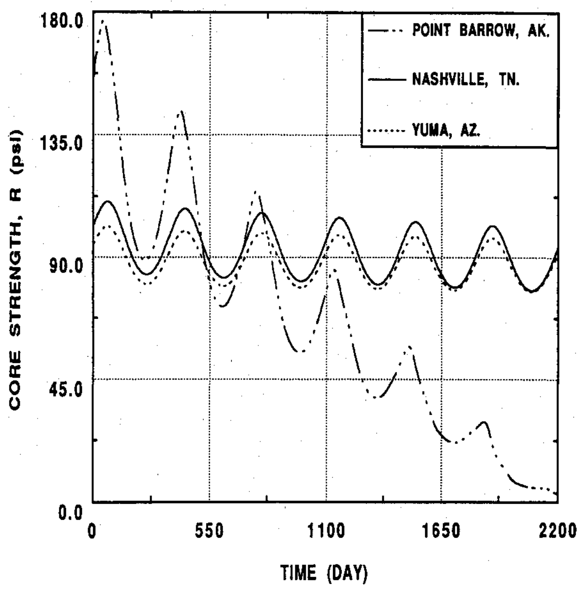

Fig. 6 Core strenth R with time at different locations (aging and damage effects are included).

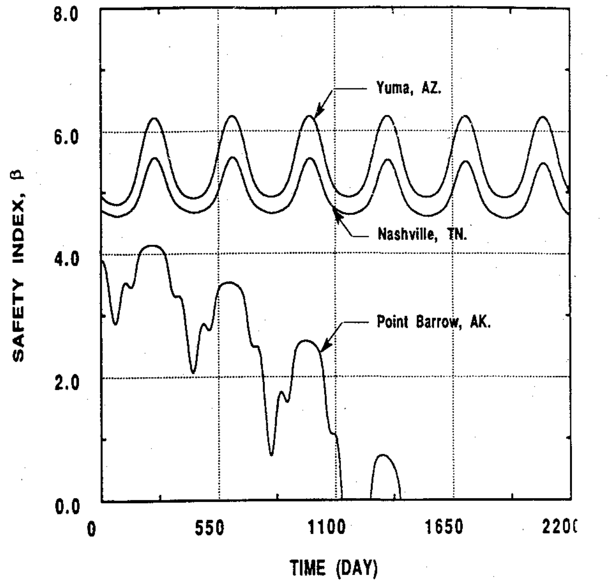

Fig. 7 Safty index β with time at different locations; strength and modulus are Weibull, and other variables are normal.

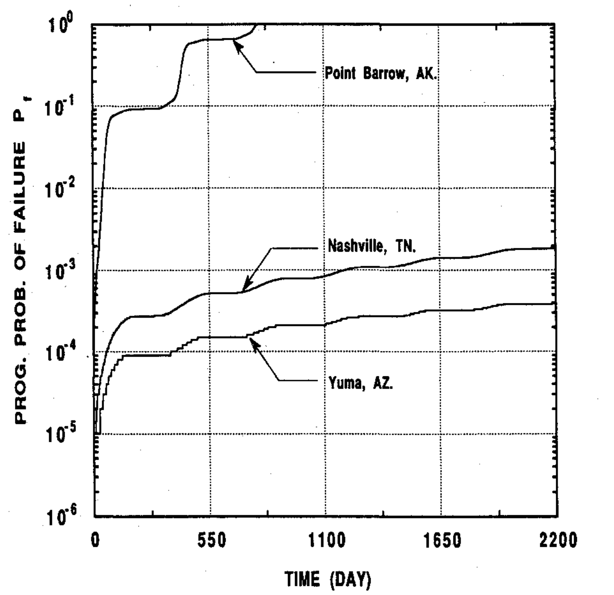

Fig. 8 Progressive probability of faliure with time at different locations; strength and modulus are Weibull, and other variables are normal.

Evaluation of the Safety Index and the Progressive Probability of Failure

Uncorrelated Nonnormal Variables (Aging and Cumulative Damage Included)

The safety index β is a measure of the reliability of a structure. A high value of β corresponds to high reliability. Using Eqs. (19–25), the safety index may be determined for each day.

The daily variations in the safety index are plotted in Fig. 7 for the three different locations, where strength and modulus have Weibull probability distributions and other variables have normal distributions. The influence of the temperature variation is clearly visible here.

Because low temperature produces high modulus and consequently high stresses, and the latter produces a high damage factor that gives rise to a significant reduction in the strength, the lowest value of β occurred at Point Barrow, AK.

The daily probability of failure may be calculated from Eq. (26), whereas the progressive probability of failure is obtained from Eqs. (27) and (28).

The progressive probability is presented in Fig. 8 again for the previous three cases. Because a low value of the safety index corresponds to high probability, the Point Barrow curve rises fastest, followed by the Nashville curve and the Yuma curve.

To illustrate the effect of probability distributions on the analysis, different probability distributions are assumed for the strength and the modulus at Nashville, TN. Results are shown in Fig. 9.

The probability of failure is less for the Weibull distributed modulus than for the lognormally distributed modulus. Therefore, if the actual probability distribution of the modulus is lognormal and the prediction was made based on Weibull, then the service life will be overestimated.

Correlated Nonnormal Variables (Aging and Cumulative Damage Included)

To illustrate the effects of correlation, three different levels of correlation are considered at the moderate site. Correlation is assumed between strength and modulus of the propellant. The Weibull probability distribution is assumed for both the strength and the modulus of the propellant, and normal probability distribution is assumed for the other variables. These cases are shown in Fig. 10.

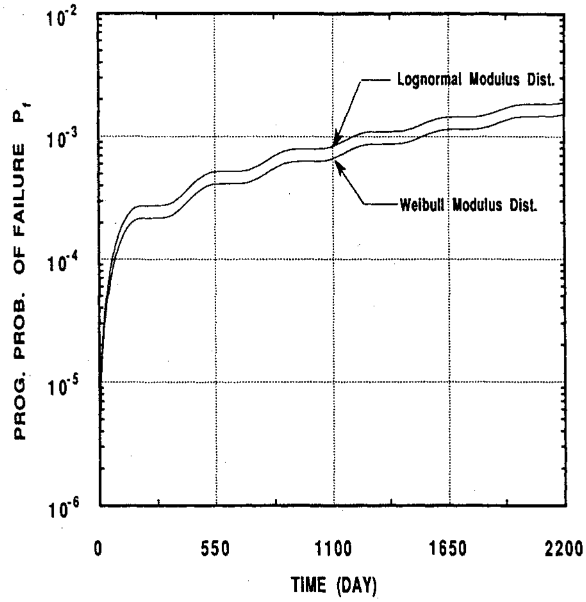

Fig. 9 Progressive probability of faliure for Weibull and lognormal modulus distributions; strength is Weibull, and other variables are normal.

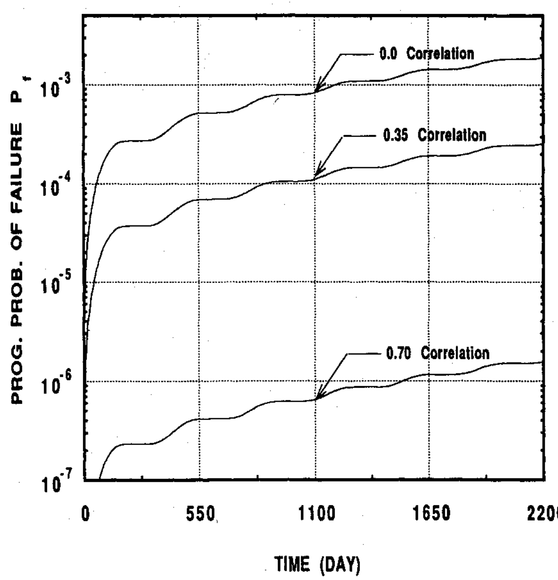

Fig. 10 Progressive probability of faliure for different levels of correlation at Nashville; strength and modulus are Weibull, and other variables are normal.

As correlation increases, the probability of failure decreases because higher stresses (higher modulus) are applied to a stronger material, whereas a weaker material is subjected to lower stresses. In the absence of correlation, such matching does not take place. The assumption of independence of variables results, therefore, in conservative estimates for reliable storage lives of motors.

Conclusions

The first-order second-moment methods of structural reliability have been applied to estimate the storage life of motors subjected to environmental temperatures. Variables with various statistical distributions and degrees of correlation have been assumed.

Under-or overestimates of the service life of rocket motors might result if the design variables are given unreasonable probability distributions. The assumption of independence between variables produces more conservative estimates than correlated variables.

Results have shown that storing rocket motors at a warm site makes them more reliable than storing them at a cold site.

A computer program entitled ROCKT2 has been developed[12] for the calculation of reliabilities and storage lives of solid propellant motors and is available to qualified users from USAMICOM/AMSMI-RD-PR, Redstone, AL 35898.

Acknowledgments

The authors gratefully acknowledge the support of this program by the U.S. Army Missile Command and the technical liaison officer J. Fisher.

References

[1]Heller, R. A., and Singh, M. P., "Thermal Storage Life of Solid Propellant Motors," *Journal of Spacecraft and Rockets*, Vol. 20, No. 2, 1983, pp. 144–149.

[2]Heller, R. A., Kamat, M. P., and Singh, M. P., "Probability of Solid Propellant Motor Failure Due to Environmental Temperatures," *Journal of Spacecraft and Rockets*, Vol. 6, No. 3, 1979, pp. 140–146.

[3]Thangjitham, S., and Heller, R. A., "Test and Evaluation of Dynamic Properties of Solid-Propellant Rocket Motor Materials," *Random Environmental Thermal Load Models and Their Effects on the Service Life of Rocket Motors*, Vol. 1, U.S. Army Missile Command, Technical Rep. CR-RD-86-8, Redstone Arsenal, AL, Oct. 1986.

[4]Zibdeh, H. S., and Heller, R. A., "Environmental Thermal Stress as a First Passage Problem," *Random Vibration—Status and Present Developments*, edited by Elishakoff and Lyon, Elsevier, New York, 1986.

[5]Zibdeh, H. S., and Heller, R. A., "Rocket Motor Service Life Calculations Based on the First Passage Method," *Journal of Spacecraft and Rockets*, Vol. 26, No. 4, 1989, pp. 279–284.

[6]Little, R. R., and Woods, H. G., "Comparison of Inert and Live Propellant Bondlines: Bondline Fabrication and Testing," U.S. Army Missile Command, Final Rep. RD-PR-92-5, Huntsville, AL, Dec. 1991.

[7]Bills, K. W., Jr., and Wiegand, J. H., "The Application of an Integrated Structural Analysis to the Prediction of Reliability," *Annals of Reliability and Maintainability*, Feb. 1970, pp. 514, 526.

[8]Layton, L. H., "Chemical Aging Studies on ANB-3066 and TP-H1011 Propellants," Air Force Rocket Propulsion Lab., Final Technical Rep. AFRPL-TR-74-16, Edwards, CA, Dec. 1974.

[9]Cost, T. L., "Service Life Predictions for Thermal Loads Using Viscoelastic Finite Element Simulation Models," U.S. Army Missile Command, Final Rep., Contract DAAH01-76-C-1069, USAMICOM-CR-79-3, Huntsville, AL, Dec. 1979.

[10]Ang, A. H. S., and Tang, W. H., *Probability Concepts in Engineering Planning and Design*, Vol. II, Wiley, New York, 1984.

[11]Thangjitham, S., and Heller, R. A., "A Comparison of Service Life Analyses," JANNAF Structures and Mechanical Behavior Committee, Huntsville, AL, March 1987.

[12]Heller, R. A., Thangjitham, S., and Janajreh, I.,"User's Guide to the Safety Index Calculation Program ROCKT2," U.S. Army Missile Command, CR-RD-PR-91-2, Redstone Arsenal, Huntsville, AL, Sept. 1991.